Nanoscale Res Lett (2007) 2:504–508
DOI 10.1007/s11671-007-9090-4

NANO EXPRESS

Surface Morphology Evolution of GaAs by Low Energy Ion Sputtering

Y. Wang · S. F. Yoon · C. Y. Ngo · J. Ahn

Received: 18 May 2007 / Accepted: 17 August 2007 / Published online: 12 September 2007

Abstract Low energy Ar^+ ion sputtering, typically below 1,200 eV, of GaAs at normal beam incident angle is investigated. Surface morphology development with respect to varying energy is analyzed and discussed. Dot-like patterns in the nanometer scale are obtained above 600 eV. As the energy approaches upper eV range regular dots have evolved. The energy dependent dot evolution is evaluated based on solutions of the isotropic Kuramoto-Sivashinsky equation. The results are in agreement with the theoretical model which describes a power law dependency of the characteristic wavelength on ion energy in the ion-induced diffusion regime.

Keywords Low energy · Ion sputtering · Surface morphology · GaAs quantum dot

Introduction

The sputtering phenomenon, which is caused by the interaction of incident particles with target surface atoms, was first observed by Grove in a dc gas discharge tube in 1852 [1]. This once regarded as undesired side effect has now been widely developed and used at large for surface cleaning and etching, thin film deposition, surface and surface layer analysis, and has long been a leading candidate for surface patterning. While ripple formation on sputtering-eroded surfaces has been observed in the 1970s [2], a self-organization process using low energy ion sputtering of semiconductor surface at normal beam incidence angle has been found recently to be capable of producing highly uniform nanoscale islands [3]. This sputtering generated surface modification is believed to be a potential alternative to techniques like Stranski-Krastanov (SK) growth and electron beam lithography that could eventually create structures in the nanometer regime exhibiting quantum properties [4, 5].

Among the III–V semiconductor compounds, GaAs quantum dots (QDs) is of great importance for fundamental quantum confinement effect studies. The GaAs/AlGaAs system, which is ideally unstrained, is particularly attractive due to the absence of strain intervention. However, being almost perfectly matched also means that GaAs QDs cannot be obtained by the SK growth mode. Nevertheless, most of the existing methods of obtaining GaAs QDs, for instance laser-induced localized interdiffusion [6], dry–wet etching [7], the use of offcut substrate [8], nanochannel alumina masks [9], in-situ etching [10] and droplet epitaxy [11] are process intensive and thus time consuming. In pursuing a promising technique to produce nanoscale GaAs dots and inspired by the sputtering induced surface morphology evolution, we present our study in this paper on GaAs surface modification by the means of ion bombardment. This research focuses on the energy-dependent surface feature development below 1,200 eV ion energy.

Theoretical Modeling

The microscopic dynamics of surface roughness and pattern formation induced by ion sputtering can be described by the noisy nonlinear Kuramoto-Sivashinsky (KS) equation [12] which defines the surface height $h(x,y,t)$ with x and y lying in the surface plane:

Y. Wang (✉) · S. F. Yoon · C. Y. Ngo · J. Ahn
School of Electrical and Electronic Engineering, Nanyang Technological University, Nanyang Avenue, Singapore 639798, Singapore
e-mail: wangyang@pmail.ntu.edu.sg

$$\frac{\partial h}{\partial t} = -v_o(\theta) + \upsilon_x \frac{\partial^2 h}{\partial x^2} + \upsilon_y \frac{\partial^2 h}{\partial y^2} - D_x \frac{\partial^4 h}{\partial x^4} - D_y \frac{\partial^4 h}{\partial y^4} - D_{xy} \frac{\partial^2}{\partial x^2}\left(\frac{\partial^2 h}{\partial y^2}\right) + \frac{\tau_x}{2}\left(\frac{\partial h}{\partial x}\right)^2 + \frac{\tau_y}{2}\left(\frac{\partial h}{\partial y}\right)^2 + \eta(x,y,t) \quad (1)$$

Here $v_o(\theta)$ is the rate of erosion of the unperturbed planar surface; υ_x and υ_y represent the effective surface tensions generated by the erosion process [13]; D_x, D_y and D_{xy} denote the surface relaxation kinetics; τ_x and τ_y describe the tilt-dependent erosion rates [14]; and $\eta(x,y,t)$ represents an uncorrelated white noise component with zero mean, which incorporates the randomness resulting from the stochastic nature of ion arrival at the surface [15]. This expression recognizes the fact that surface relaxation is governed by two different diffusion processes. The terms with coefficients D_x and D_y are thermally activated. Their smoothing rates are based on mass transport on the surface. $D_{xy}\partial^2/\partial x^2(\partial^2 h/\partial y^2)$, the sputtering induced diffusion, is regarded as a smoothing contribution in the morphology evolution without mass transport.

In general, ion bombardment provokes an anisotropic instability giving rise to characteristic ripple patterns [13]. In a very special case where the ion beam impinges perpendicular to the target surface, coefficients in Eq. (1) become isotropic and a regular matrix of dots is expected to be formed [16]. The temporal surface height evolution can then be expressed as an isotropic KS equation [5]:

$$\frac{\partial h}{\partial t} = -v_o(\theta) + \upsilon \nabla^2 h - D\nabla^4 h + \frac{\tau}{2}(\nabla h)^2 + \eta(x,y,t) \quad (2)$$

with

$$\upsilon = -\frac{a\beta^2}{2\alpha^2}\left[\frac{J\varepsilon p}{\sqrt{2\pi}\alpha}\exp\left(-\frac{a^2}{2\alpha^2}\right)\right] \quad (3)$$

where J is the ion current density, p the proportionality factor coupling the energy deposited to the erosion rate [13], ε the total energy deposited, and a the average depth of energy deposition. α and β are the widths of the distribution parallel and perpendicular to the beam direction, respectively [10] (generally a, α, and β are comparable in magnitude [13]). The diffusion coefficient D in Eq. (2), which is assumed isotropic, includes all diffusion coefficients, i.e., the thermal diffusion (D_t) and effective sputtering induced diffusion (D_{eff}).

$$D_t = D_o \exp\left(\frac{-E_a}{k_B T}\right) \quad (4)$$

$$D_{\text{eff}} = \frac{a\beta^4}{8\alpha^2}\left[\frac{J\varepsilon p}{\sqrt{2\pi}\alpha}\exp\left(-\frac{a^2}{2\alpha^2}\right)\right] \quad (5)$$

Here E_a is the activation energy, k_B the Boltzmann's constant, and T the temperature. In Eq. (2), the balance of the unstable erosion term ($\upsilon\nabla^2 h$) and the surface diffusion term ($-D\nabla^4 h$) acting to smooth the surface, generates dots with characteristic wavelength that equals:

$$l_c = 2\pi\sqrt{2\left(\frac{D}{|\upsilon|}\right)} \quad (6)$$

It is difficult to differentiate the two diffusion mechanisms when they simultaneously co-exist. However, at low temperature and comparably high ion energy, D_t is negligibly small compared to D_{eff}, and the effective ion-induced diffusion should dominate over thermal diffusion [10]. Hence, based on Eqs. (3), (5), and (6), l_c becomes:

$$l_c = \sqrt{2}\pi\beta \quad (7)$$

Because β, the lateral width of the energy deposited, is related to the sputtering energy (ε) by $\beta \propto \varepsilon^{2m}$ [5], the characteristic wavelength is related to the sputtering energy by a power law [10]:

$$l_c \propto \sqrt{2}\pi\varepsilon^{2m} \quad (8)$$

The parameter m is between 0 and 1. $m = 1$ holds for Rutherford scattering. In the lower-keV and upper eV region, $m = 1/3$ should be adequate [17]. Equation (8) which implies the characteristic wavelength, is a strong function of the ion energy and independent of other parameters, for instance the ion beam flux and sample surface temperature, in the case of sputtering induced diffusion.

Experiment Details

The samples used are commercial GaAs (100) wafers. A Veeco ion source is used to provide the Ar^+ ion beam, which impinges perpendicularly onto the sample surface. The process chamber pressure is maintained below 4×10^{-4} Torr by a turbo pump. All samples are sputtered for 300 s with the ion current kept at 10 mA which is equivalent to 8.8×10^{15} cm^{-2} s^{-1} beam flux. The surface morphology induced by ion sputtering is analyzed ex situ by a Digital Instruments atomic force microscopy (AFM). The cantilever used has 5 nm guaranteed tip radius of curvature.

Results and Discussion

Figure 1 shows the AFM images of sputtered GaAs surfaces with sputtering energies of 250, 600, and 1,200 eV respectively. These images represent different observed surface structural development regimes. The surface

morphology evolution can be summarized as follows: In the low eV range, no visible feature appears except for surface roughening (Fig. 1a). Above the mid-eV energy dot-like patterns start forming, but they are accompanied by the presence of irregular and rough features together with some conjoined dots forming bigger coalesced islands (Fig. 1b). This partially chaotic surface state is gradually suppressed as the sputtering energy becomes stronger and exceeds 1 keV. Separations between dots can clearly be seen up to this regime (Fig. 1c). The sputtering-created dots at 1,200 eV are particularly analyzed. The extracted dot height and dot base width are plotted in Fig. 2. Statistically the dots are 22 nm in base width, 2.3 nm in height, and 6×10^{10} cm^{-2} in density. The two histograms in Gaussian-like bell shapes suggest considerably good uniformity and regularity of the dot distribution. The three dimensional (3D) surface image depicted in Fig. 3 reveals well shaped nanoscale dots with only a few of them conjoined.

In order to elucidate the dot formation mechanism, recall Eq. (8). Since the effects of background gas pressure on ion beam energy and momentum have generally been ignored in ion sputtering applications [18], the ion energy supplied by the controller can be treated as the actual energy that the ion beam carries when it hits the sample surface. By putting together the surface characteristic wavelength obtained in the 2D power spectral density (PSD) analysis as described in Ref. [19] and the ion energy in a double logarithm graph (Fig. 4), the energy dependent dot evolution on GaAs surface can be readily discussed. Due to the presence of uniformity and stochastic roughness, the obtained characteristic wavelength spreads in relatively large scale at 600 eV. As the energy approaches 1,200 eV this spread becomes smaller corresponding to shorter error bars. A linear fit of the data points yields a slope of $2m = 0.78$, or $m = 0.39$. This is in good agreement with the sputtering theory that in the lower energy range, the characteristic QD base width increases with ion energy according to the power law in Eq. (8) with $m \sim 1/3$ [17]. This suggests that the effective ion induced diffusion dominates over thermal diffusion in this energy range for the dot formation on GaAs.

For energies lower than 600 eV, no dot-like patterns are observed. In other words, the threshold energy for GaAs nanoscale dots formation is near 600 eV for 300 s Ar^+ sputtering. Even though the threshold energy has so far eluded theoretical proof, its existence and characteristic can still be predicted and justified based on current sputtering theory. From what has been reported by Facsko et al. [10] and Bobek et al. [19], there exists an onset time to let the sputtered surface enter the early time QD formation regime at a fixed sputtering energy. This can be interpreted as: for a given sputtering time

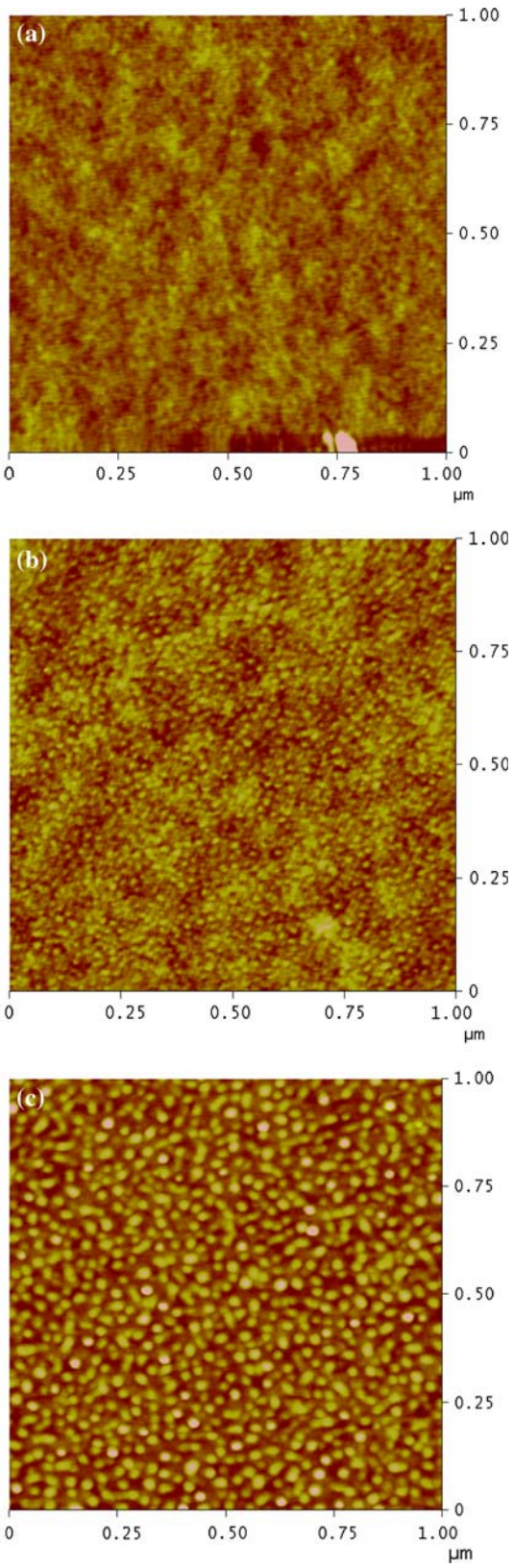

Fig. 1 AFM images of Ar^+ sputtered GaAs(100) surfaces with ion energies of (**a**) 250 eV, (**b**) 600 eV and (**c**) 1,200 eV

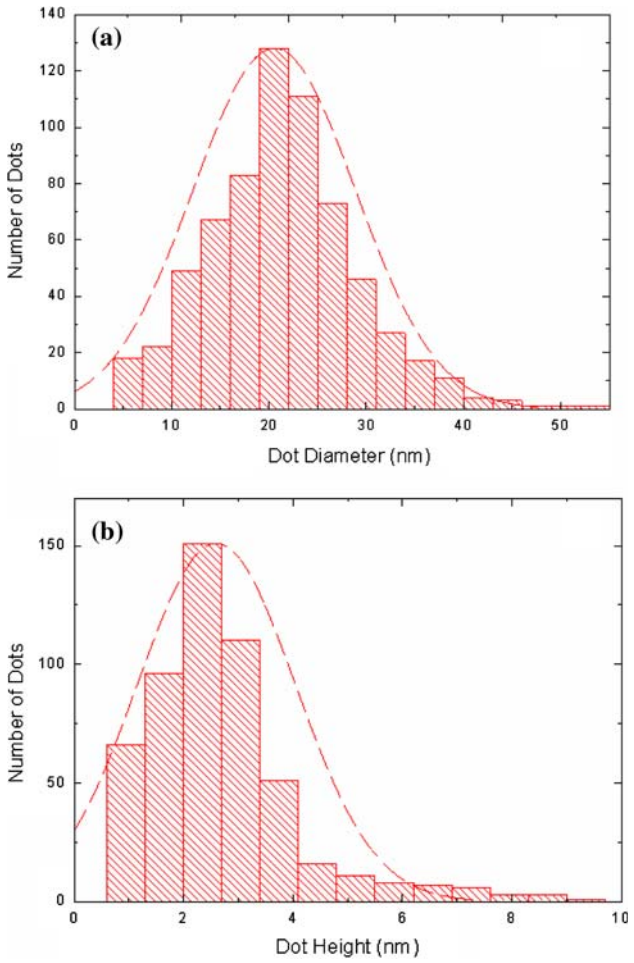

Fig. 2 Histograms of (**a**) base diameter and (**b**) height distributions of the GaAs nanoscale dots formed at 1,200 eV

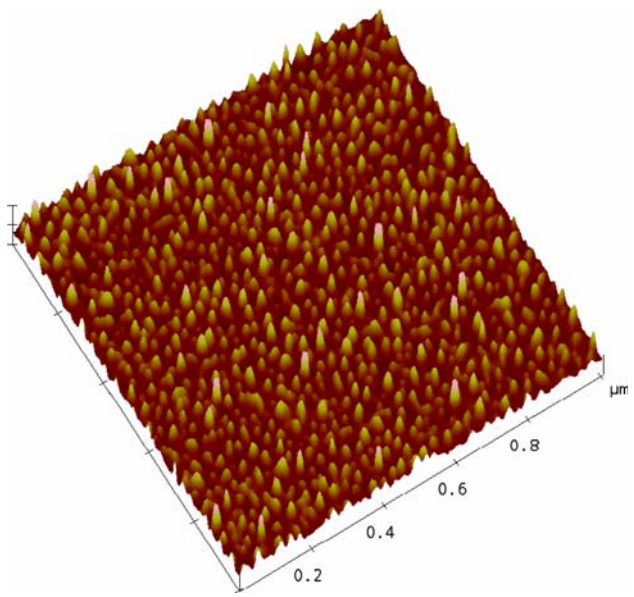

Fig. 3 3D surface plot of the GaAs nanoscale dots formed at 1,200 eV

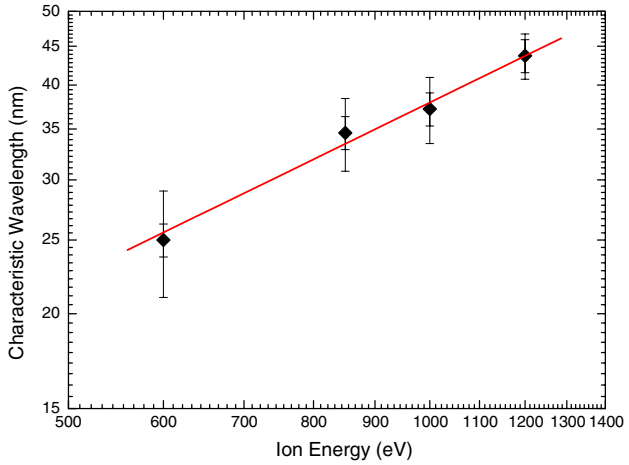

Fig. 4 Energy dependent dot characteristic wavelength evolution

and varying sputtering energy, there exists the possibility that this sputtering duration is not long enough for some low sputtering energies to initiate dot formation, or these energies are below the threshold energy. Sputtering time and energy are two relative concepts. A shorter sputtering time could need higher sputtering energy to achieve the same outcome as in longer sputtering time but lower sputtering energy. Furthermore, by putting this temporal concept into the energy dependency, it is not difficult to conclude that in the ion induced diffusion regime, the ion energy against characteristic wavelength profile can be shifted by the sputtering time. With the same ion energy, longer sputtering time leads to smaller threshold energy and longer characteristic wavelength, yet the profile moves upwards.

Conclusions

In summary, the Ar^+ sputtering induced GaAs(100) surface morphology evolution below 1,200 eV ion energy is investigated. The sputtered surface is examined and analyzed by AFM. In the low eV energy range, no regular surface patterns are observed. Above the mid-eV energy, typically 600 eV in this series of experiment, dot-like islands mixed with irregularities start developing and grow with increasing ion energy. The measured dot characteristic wavelength exhibits a power law dependence on the sputtering energy. The factor m in Eq. (8) has been graphically determined to be 0.39. This value is theoretically reasonable because in the lower eV and upper keV range factor m is typically around 1/3.

References

1. K. Wasa, M. Kitabatake, H. Adachi, Thin Film Materials Technology - Sputtering of Compound Materials. William Andrew Publishing/Noyes. p. 71 (2004)
2. F. Vasiliu, I.A. Teodorescu, F. Glodeanu, J. Mater. Sci. **10**, 399 (1975)

3. S. Facsko, T. Dekorsy, C. Koerdt, C. Trappe, H. Kurz, A. Vogt, H. Hartnagel, Science **285**, 155 (1999)
4. S. Facsko, T. Dekorsy, C. Trappe, H. Kurz, Microelectron. Eng. **53**, 245 (2000)
5. S. Facsko, H. Kurz, T. Dekorsy, Phys. Rev. B **63**, 165329 (2001)
6. K. Brunner, U. Bockelmann, G. Abstreiter, M. Walther, G. Bohm, G. Trankle, G. Weimann, Phys. Rev. Lett. **69**, 3216 (1992)
7. X.H. Wang, A.M. Song, J. Liu, W.C. Cheng, G.H. Li, C.F. Li, Y.X. Li, J.Z. Yu, Proc. SPIE **3899**, 147 (1999)
8. T. Tsujikawa, S. Mori, H. Watanabe, M. Yoshita, H. Akiyama, V. Dalen, K. Onabe, H. Yaguchi, Y. Shiraki, R. Ito, Physica E **7**, 308 (2000)
9. X. Mei, M. Blumin, M. Sun, D. Kim, Z.H. Wu, H.E. Ruda, Q.X. Guo, Appl. Phys. Lett. **82**, 967 (2003)
10. A. Rastelli, S. Stufler, A. Schliwa, R. Songmuang, C. Manzano, G. Costantini, K. Kern, A. Zrenner, D. Bimberg, O.G. Schmidt, Phys. Rev. Lett. **92**, 166104 (2004)
11. T. Mano, T. Kuroda, M. Yamagiwa, G. Kido, K. Sakoda, N. Koguchi, Appl. Phys. Lett. **89**, 183102 (2006)
12. Y. Kuramoto, Chemical Oscillations, Waves, and Turbulence (Springer, Berlin, 1984); G.I. Sivashinsky, Acta Astronaut. **4**, 1177 (1997); G.I. Sivashinsky and D.M. Michelson, Prog. Theor. Phys. **63**, 2112 (1980)
13. R.M. Bradley, J.M.E. Harper, J. Vac. Sci. Technol. A **6**, 2390 (1988)
14. S. Park, B. Kahng, H. Jeong, A.-L. Barabasi, Phys. Rev. Lett. **83**, 3486 (1999)
15. M. A. Makeev, A.-L. Barabasi, Appl. Phys. Lett. **71**, 2800 (1997)
16. G. Carter, V. Vishnyakov, Phys. Rev. Lett. **72**, 3040 (1994)
17. P. Sigmund, Phys. Rev. **184**, 383 (1969)
18. H.R. Kaufman, J.M.E. Harper, J.J. Cuomo, J. Vac. Sci. Technol. **21**, 737 (1982)
19. T. Bobek, S. Facsko, H. Kurz, Phys. Rev. B **68**, 085324 (2003)